

# SRG operator evolution

A. J. Tropiano<sup>1</sup>, S. K. Bogner<sup>2</sup>, R. J. Furnstahl<sup>1</sup>

<sup>1</sup>*Department of Physics, The Ohio State University, Columbus, OH 43210, USA*

<sup>2</sup>*National Superconducting Cyclotron Laboratory and Department of Physics and Astronomy,  
Michigan State University, East Lansing, MI 48824, USA*

(Dated: August 27, 2019)

## Abstract

Brief description of project.

## CONTENTS

I. Introduction	3
II. Mathematical/computational details	3
A. Building SRG unitary transformations	3
B. Momentum projection operator: $a_q^\dagger a_q$	3
C. Momentum distribution function: $\phi^2(k)$	4
III. Results	4
A. Entem-Machleidt N <sup>3</sup> LO non-local potential	4
B. RKE N <sup>3</sup> LO and N <sup>4</sup> LO semi-local potentials	8
C. Gezerlis N <sup>2</sup> LO local potentials	16
References	19

## I. INTRODUCTION

Results on SRG-evolved operators from several NN potentials.

- How operators evolve from band- and block-diagonal SRG transformations.
- Operator evolution for different potentials (regulators, chiral order, etc.)

## II. MATHEMATICAL/COMPUTATIONAL DETAILS

### A. Building SRG unitary transformations

Diagonalize initial and evolved Hamiltonians which we will call  $H(0)$  and  $H(s)$ , respectively. This gives  $\psi_\alpha(0)$  and  $\psi_\alpha(s)$  for each eigenvalue indexed by  $\alpha$ . Then the SRG unitary transformation can be computed by taking a sum over outer products of the evolved and initial wave functions:

$$U(s) = \sum_{\alpha=1}^N |\psi_\alpha(s)\rangle \langle \psi_\alpha(0)|, \quad (1)$$

where  $N$  is the dimension of the Hamiltonian matrix. Here the weights are factored into the wave functions, thus  $U(s)$  is unitless.

To evolve operators, we simply apply  $U(s)$ :

$$O(s) = U(s)O(0)U^\dagger(s), \quad (2)$$

where  $O(0)$  is the bare operator.

### B. Momentum projection operator: $a_q^\dagger a_q$

Applying  $a_q^\dagger a_q$  to a wave function  $\psi(k)$  returns  $\psi(q)$ . For the discrete case,  $\psi(k_i)$  is an  $N \times 1$  vector and  $a_q^\dagger a_q(k_i, k_j)$  is an  $N \times N$  matrix where  $i, j = 1, \dots, N$ . Then  $a_q^\dagger a_q$  acting on  $\psi(k)$  is a matrix multiplication, implying a continuous integration over  $d^3k/(2\pi)^3 = 2/(\pi k^2 dk)$  in spherical coordinates. Therefore, we include a factor of  $\pi/(2k_i k_j \sqrt{w_i w_j})$  in  $a_q^\dagger a_q(k_i, k_j)$  where  $w$  represents the momentum weights. In matrix form,

$$a_q^\dagger a_q(k_i, k_j) = \frac{\pi \delta_{k_i q} \delta_{k_j q}}{2k_i k_j \sqrt{w_i w_j}}, \quad (3)$$

which has units  $\text{fm}^3$ . To evolve operators, we apply  $U(s)$  at this point. For mesh-independent figures, we must divide by an additional factor of  $k_i k_j \sqrt{w_i w_j}$ .

### C. Momentum distribution function: $\phi^2(k)$

We diagonalize the Hamiltonian for eigenvectors  $\psi_\alpha$ . In the  ${}^3S_1$ - ${}^3D_1$  coupled channel, the S-component is given by  $\psi_\alpha[:N]$  and the D-component by  $\psi_\alpha[N:]$  where  $N$  is the length of the momentum mesh. Then the momentum distribution of the state  $\alpha$  is given by,

$$|\phi_\alpha(k)|^2 = |\psi_\alpha[:N]|^2 + |\psi_\alpha[N:]|^2. \quad (4)$$

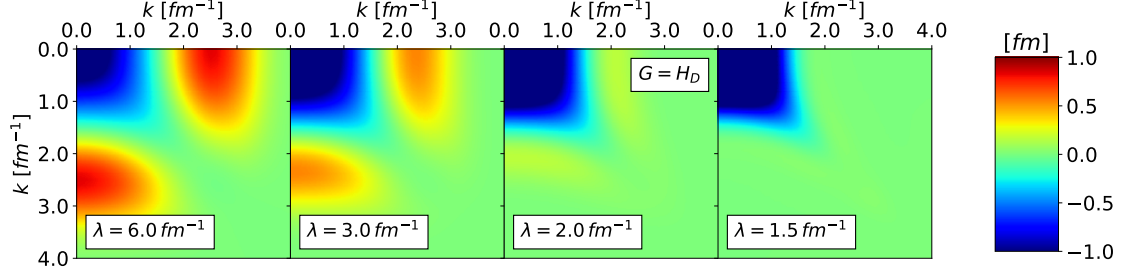
This satisfies the normalization condition  $\sum_{i=1}^N |\phi(k_i)|^2 = 1$ , implying that the factor  $k^2 dk$  (or in the discrete case,  $k_i^2 w_i$ ) is factored into the wave function. For mesh-independent figures, divide by  $k_i^2 w_i$ .

## III. RESULTS

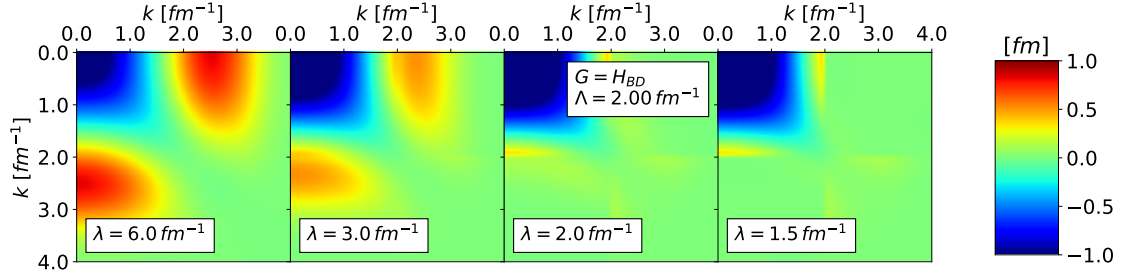
Organize this according to the figures. Format should be description of the calculation (previous section), followed by the figure, followed by takeaways.

### A. Entem-Machleidt $\text{N}^3\text{LO}$ non-local potential

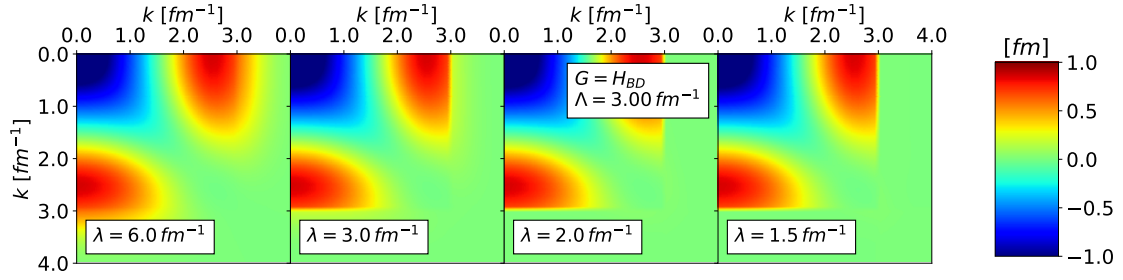
Non-local potential from [1].



(a)

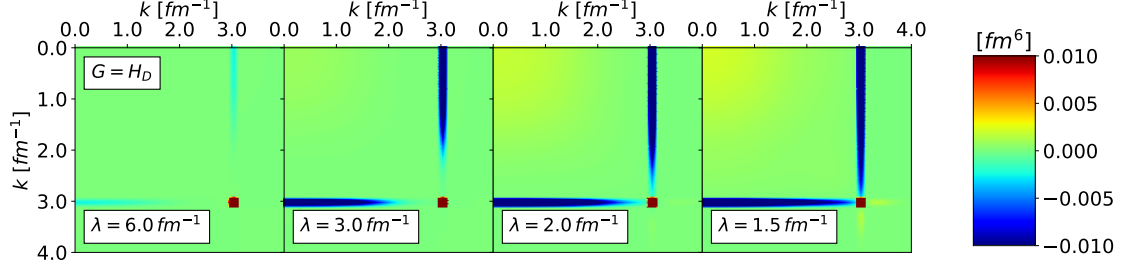


(b)

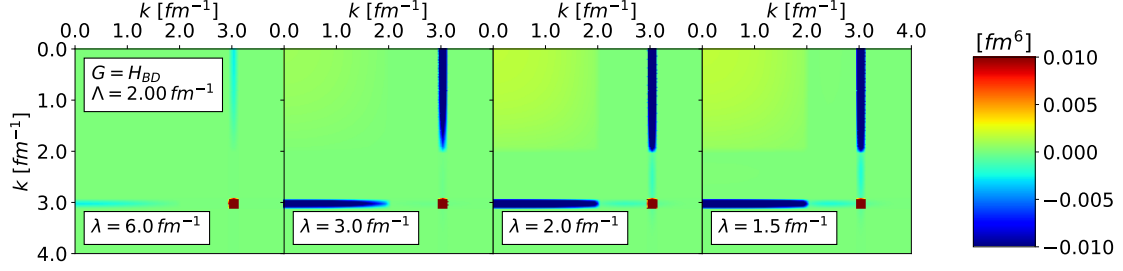


(c)

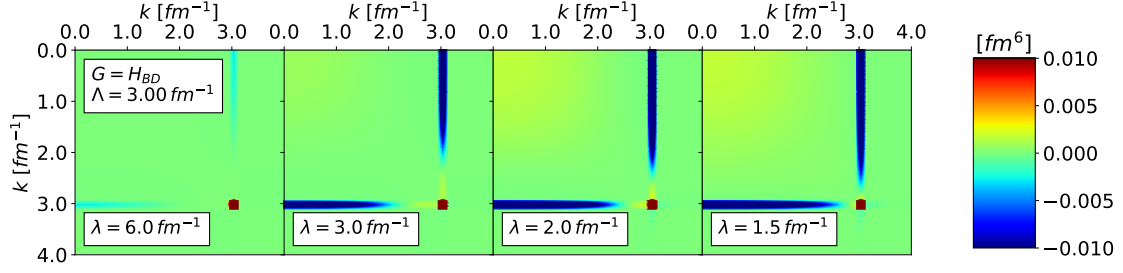
FIG. 1: Matrix elements of the Entem-Machleidt N<sup>3</sup>LO non-local potential  $V_\lambda(k, k')$  SRG-evolving in  $\lambda$  right to left under transformations with the Wegner generator (a) and block-diagonal generators decoupling at  $\Lambda = 2$  and  $3 \text{ fm}^{-1}$  (b and c).



(a)



(b)



(c)

FIG. 2: Matrix elements of  $\langle k|a_q^\dagger a_q|k' \rangle$  SRG-evolving in  $\lambda$  right to left under transformations from the Entem-Machleidt N<sup>3</sup>LO non-local potential with the Wegner generator (a) and block-diagonal generators decoupling at  $\Lambda = 2$  and  $3 \text{ fm}^{-1}$  (b and c). Here  $q = 3 \text{ fm}^{-1}$ .

- The top row of Fig. 2 should match the top row in Fig. 4 of [2].
- Smeared delta function comment.
- Compared block-diagonal to Wegner.
- Another note about block-diagonal.

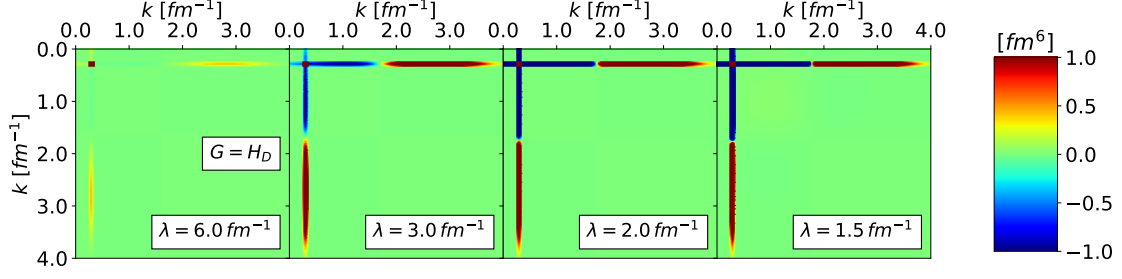


FIG. 3: Matrix elements of  $\langle k|a_q^\dagger a_q|k'\rangle$  SRG-evolving in  $\lambda$  right to left under transformations from the Entem-Machleidt N<sup>3</sup>LO non-local potential with the Wegner generator. Here  $q = 0.3 \text{ fm}^{-1}$ .

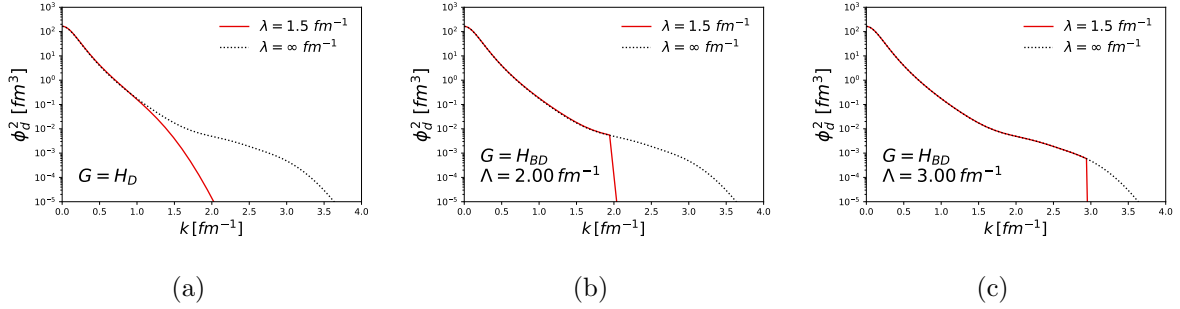


FIG. 4: Momentum probability densities of the deuteron SRG-evolving the wave function to  $\lambda = 1.5 \text{ fm}^{-1}$  from the Entem-Machleidt N<sup>3</sup>LO non-local potential with the Wegner generator (a) and block-diagonal generators decoupling at  $\Lambda = 2$  and  $3 \text{ fm}^{-1}$  (b and c). The black dotted line corresponds to the momentum probability density of the initial deuteron wave function.

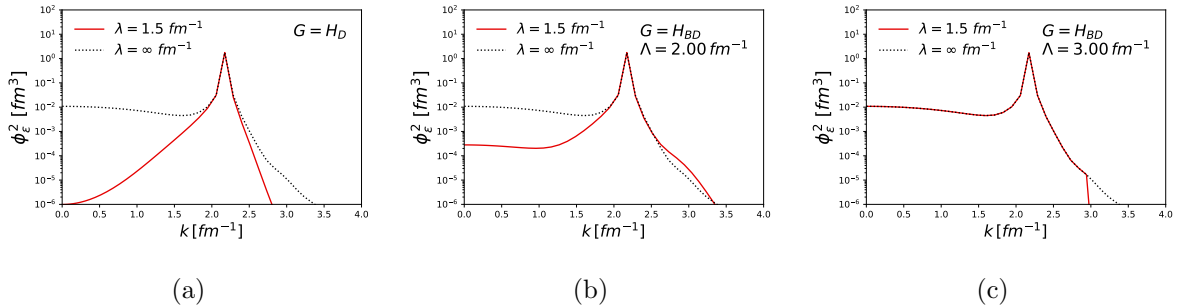
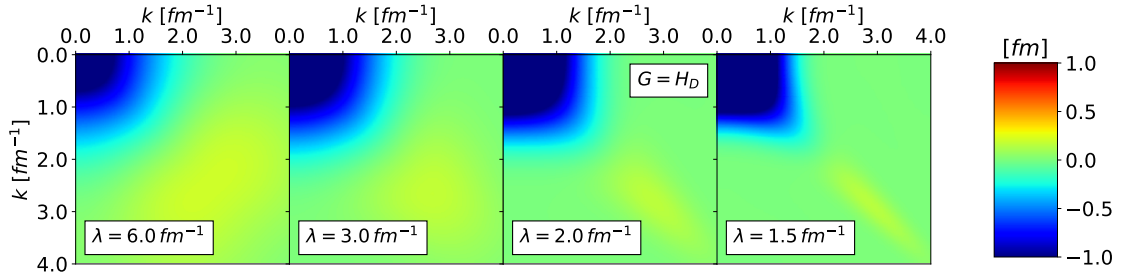


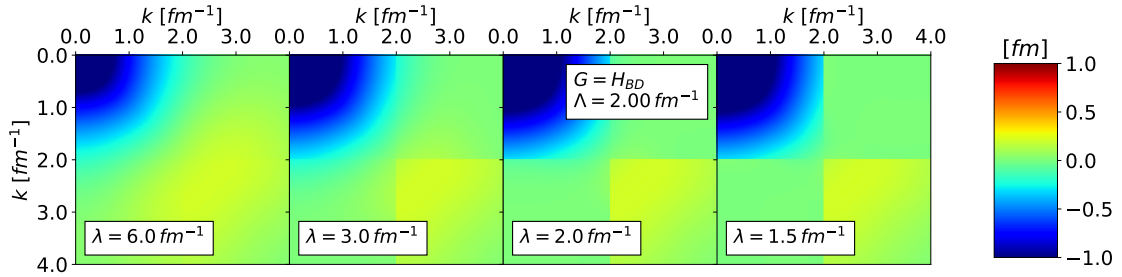
FIG. 5: Momentum probability densities of the continuum state at  $\epsilon \approx 200 \text{ MeV}$  SRG-evolving the wave function to  $\lambda = 1.5 \text{ fm}^{-1}$  from the Entem-Machleidt N<sup>3</sup>LO non-local potential with the Wegner generator (a) and block-diagonal generators decoupling at  $\Lambda = 2$  and  $3 \text{ fm}^{-1}$  (b and c). The black dotted line corresponds to the initial momentum probability density.

## B. RKE N<sup>3</sup>LO and N<sup>4</sup>LO semi-local potentials

Add takeaways for these figures. Semi-local potentials from [3].



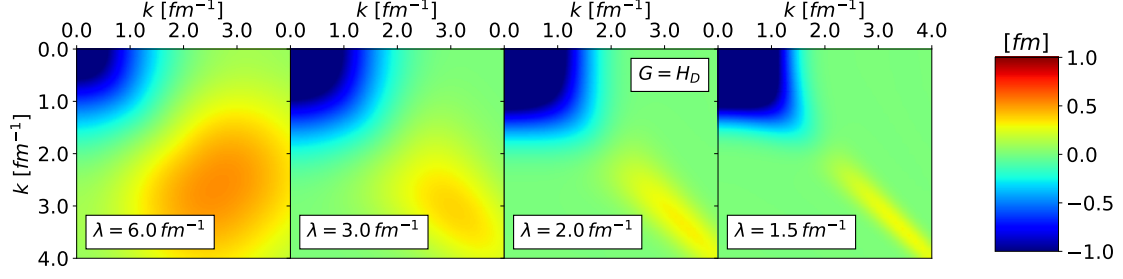
(a)



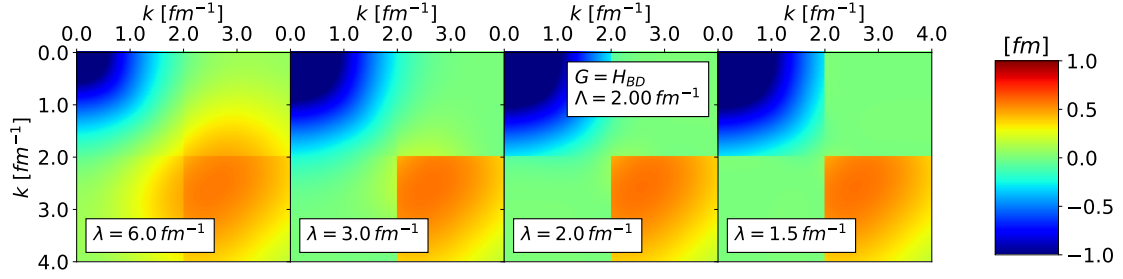
(b)

FIG. 6: Matrix elements of the RKE N<sup>3</sup>LO semi-local potential  $V_\lambda(k, k')$  SRG-evolving in  $\lambda$  right to left under transformations with the Wegner generator (a) and block-diagonal generator decoupling at  $\Lambda = 2 \text{ fm}^{-1}$  (b). Here the EFT cutoff is 450 MeV.



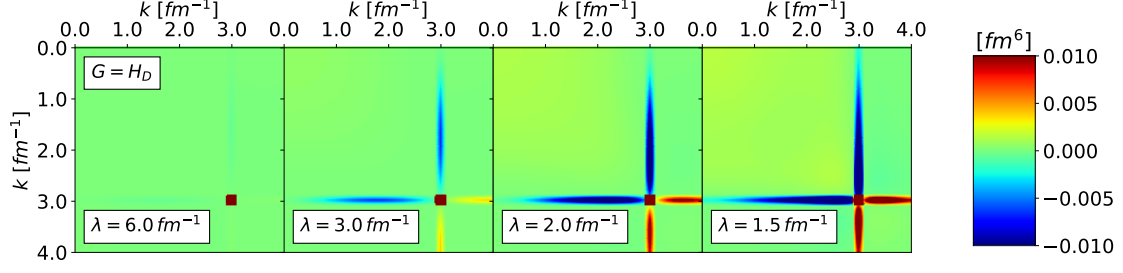


(a)

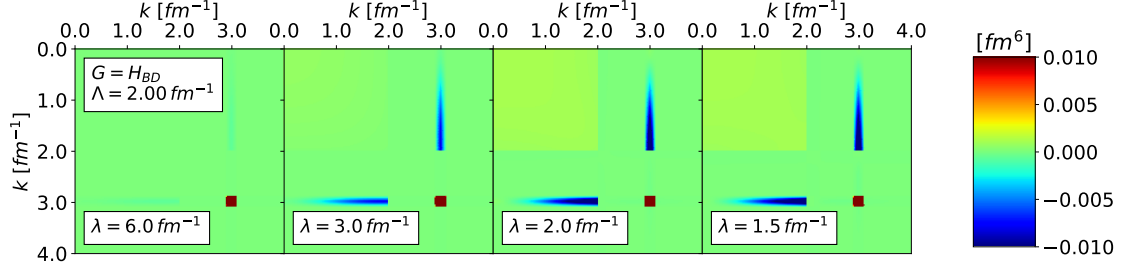


(b)

FIG. 7: Matrix elements of the RKE N<sup>3</sup>LO semi-local potential  $V_\lambda(k, k')$  SRG-evolving in  $\lambda$  right to left under transformations with the Wegner generator (a) and block-diagonal generator decoupling at  $\Lambda = 2 \text{ fm}^{-1}$  (b). Here the EFT cutoff is 500 MeV.

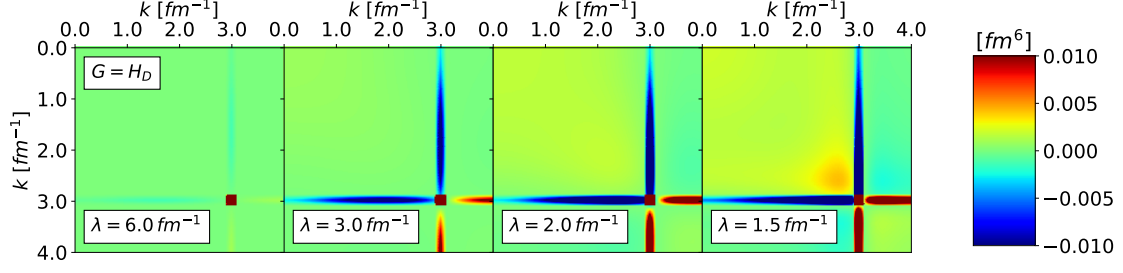


(a)

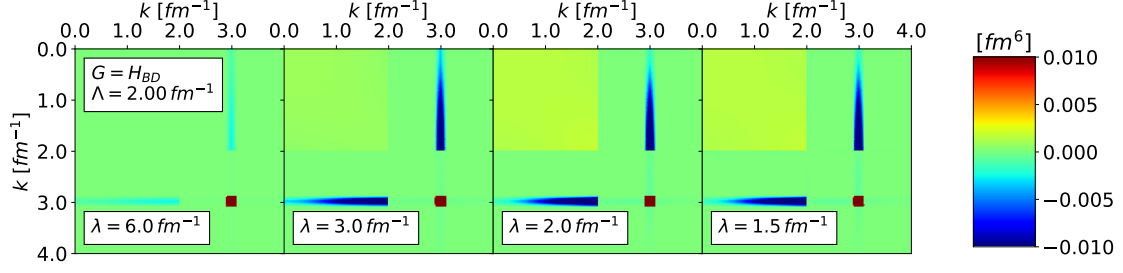


(b)

FIG. 8: Matrix elements of  $\langle k|a_q^\dagger a_q|k'\rangle$  SRG-evolving in  $\lambda$  right to left under transformations from the RKE N<sup>3</sup>LO semi-local potential with the Wegner generator (a) and block-diagonal generator decoupling at  $\Lambda = 2 \text{ fm}^{-1}$  (b). Here  $q = 3 \text{ fm}^{-1}$  and the EFT cutoff is 450 MeV.

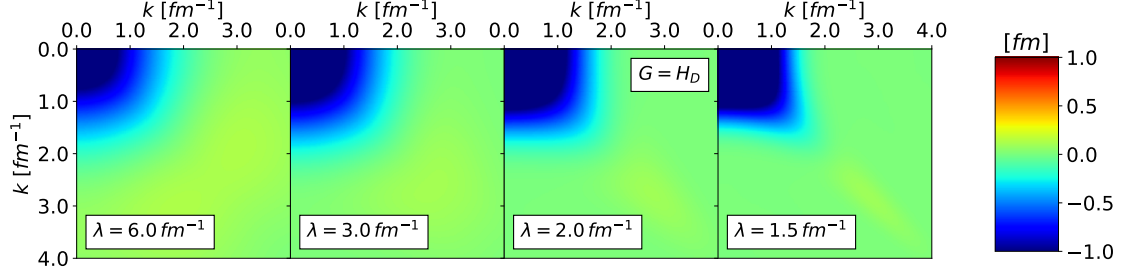


(a)

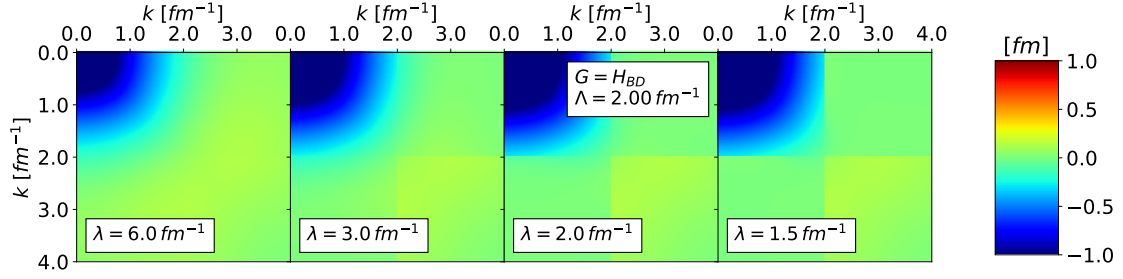


(b)

FIG. 9: Matrix elements of  $\langle k | a_q^\dagger a_q | k' \rangle$  SRG-evolving in  $\lambda$  right to left under transformations from the RKE N<sup>3</sup>LO semi-local potential with the Wegner generator (a) and block-diagonal generator decoupling at  $\Lambda = 2 \text{ fm}^{-1}$  (b). Here  $q = 3 \text{ fm}^{-1}$  and the EFT cutoff is 500 MeV.

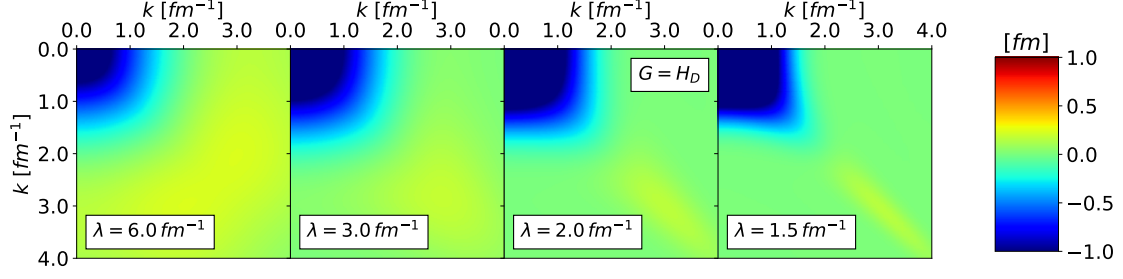


(a)

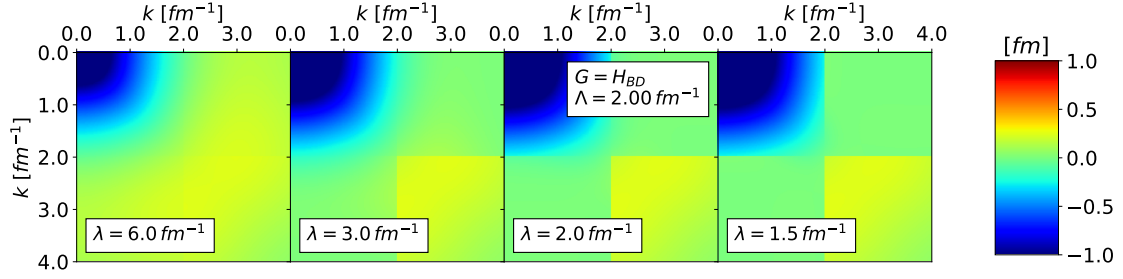


(b)

FIG. 10: Matrix elements of the RKE N<sup>4</sup>LO semi-local potential  $V_\lambda(k, k')$  SRG-evolving in  $\lambda$  right to left under transformations with the Wegner generator (a) and block-diagonal generator decoupling at  $\Lambda = 2 \text{ fm}^{-1}$  (b). Here the EFT cutoff is 450 MeV.

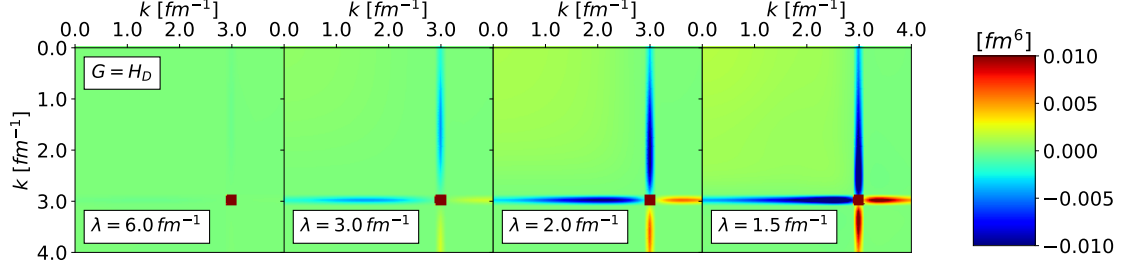


(a)

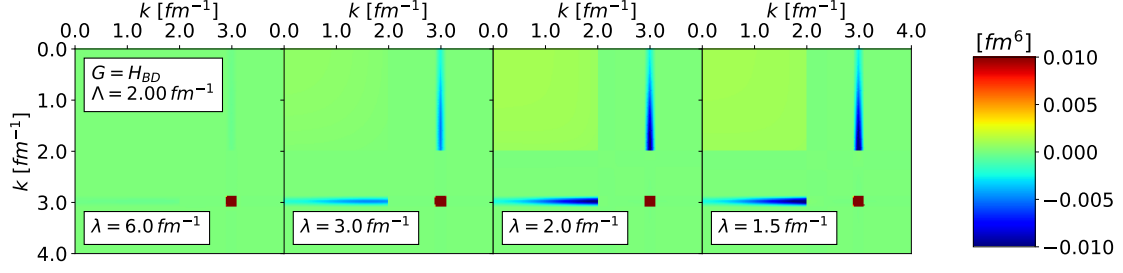


(b)

FIG. 11: Matrix elements of the RKE N<sup>4</sup>LO semi-local potential  $V_\lambda(k, k')$  SRG-evolving in  $\lambda$  right to left under transformations with the Wegner generator (a) and block-diagonal generator decoupling at  $\Lambda = 2 \text{ fm}^{-1}$  (b). Here the EFT cutoff is 500 MeV.

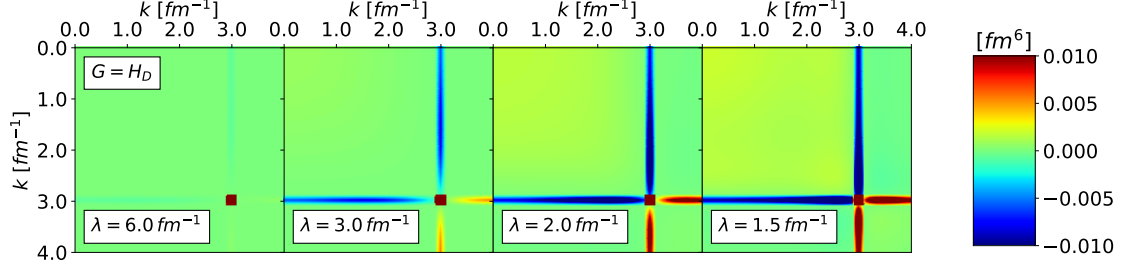


(a)

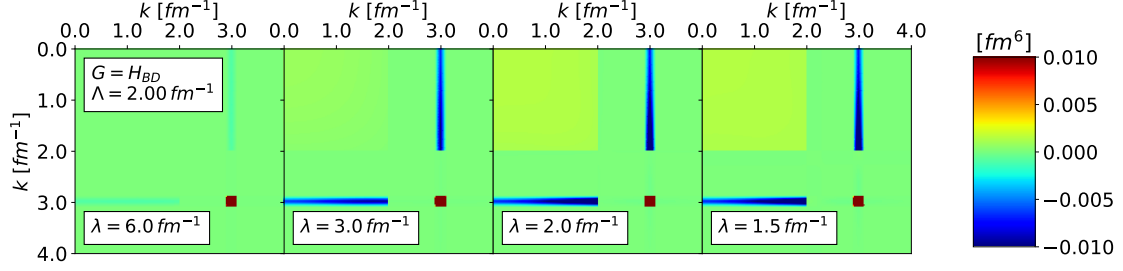


(b)

FIG. 12: Matrix elements of  $\langle k|a_q^\dagger a_q|k'\rangle$  SRG-evolving in  $\lambda$  right to left under transformations from the RKE N<sup>4</sup>LO semi-local potential with the Wegner generator (a) and block-diagonal generator decoupling at  $\Lambda = 2 \text{ fm}^{-1}$  (b). Here  $q = 3 \text{ fm}^{-1}$  and the EFT cutoff is 450 MeV.

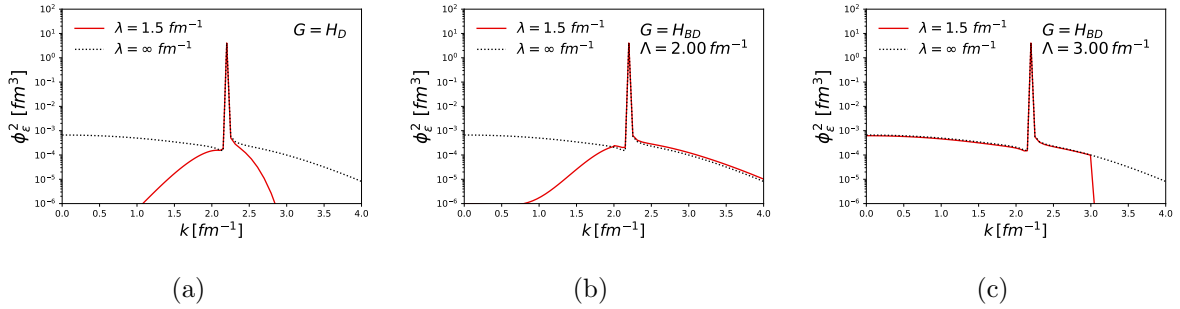


(a)



(b)

FIG. 13: Matrix elements of  $\langle k | a_q^\dagger a_q | k' \rangle$  SRG-evolving in  $\lambda$  right to left under transformations from the RKE N<sup>4</sup>LO semi-local potential with the Wegner generator (a) and block-diagonal generator decoupling at  $\Lambda = 2 \text{ fm}^{-1}$  (b). Here  $q = 3 \text{ fm}^{-1}$  and the EFT cutoff is 500 MeV.



(a)

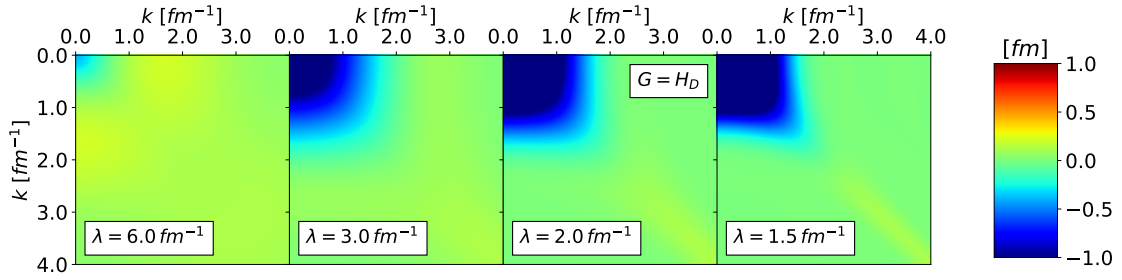
(b)

(c)

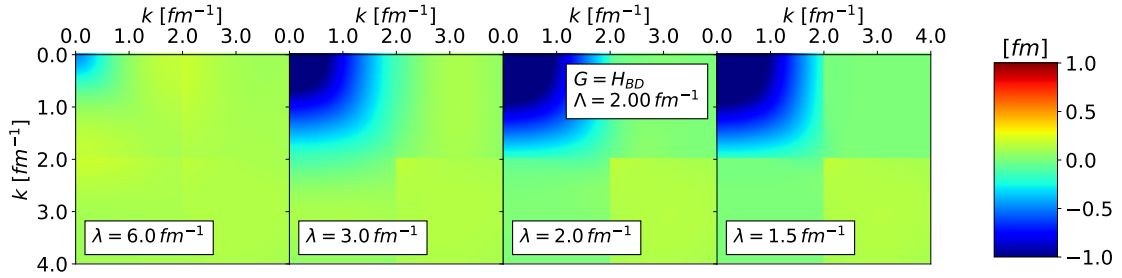
FIG. 14: Momentum probability densities of the continuum state at  $\epsilon \approx 200 \text{ MeV}$  SRG-evolving the wave function to  $\lambda = 1.5 \text{ fm}^{-1}$  from the RKE N<sup>4</sup>LO semi-local potential with the Wegner generator (a) and block-diagonal generators decoupling at  $\Lambda = 2$  and  $3 \text{ fm}^{-1}$  (b and c). The black dotted line corresponds to the initial momentum probability density. Here the EFT cutoff is 450 MeV.

### C. Gezerlis N<sup>2</sup>LO local potentials

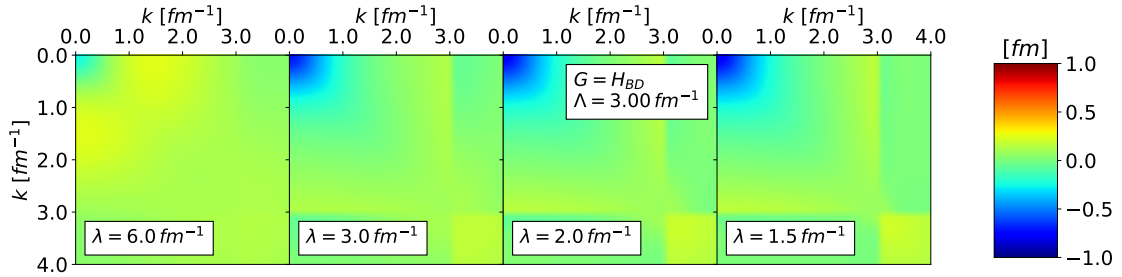
Add takeaways for these figures. Local potentials from [4].



(a)



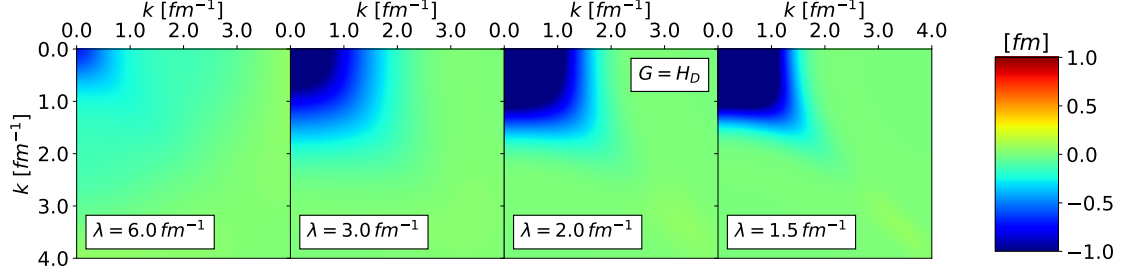
(b)



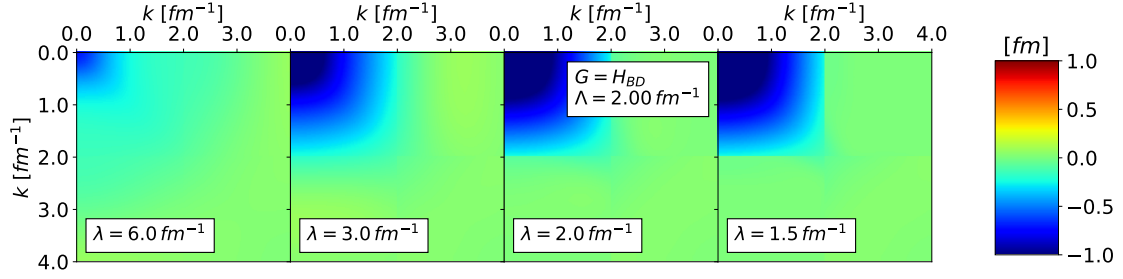
(c)

FIG. 15: Matrix elements of the Gezerlis et al. N<sup>2</sup>LO local potential  $V_\lambda(k, k')$  SRG-evolving in  $\lambda$  right to left under transformations with the Wegner generator (a) and block-diagonal generators decoupling at  $\Lambda = 2$  and  $3 \text{ fm}^{-1}$  (b and c). Here the EFT cutoff is 1 fm.



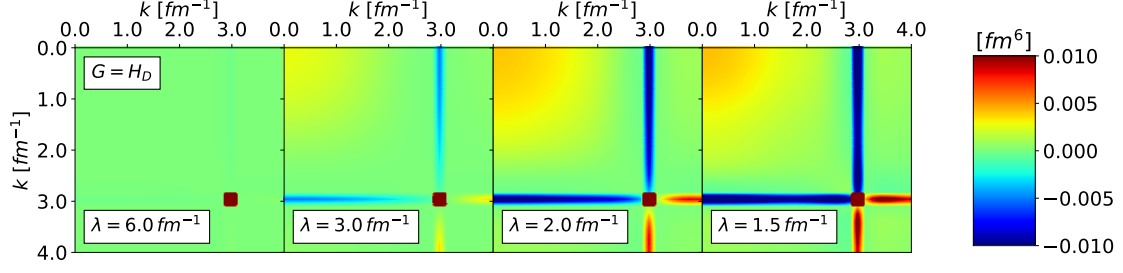


(a)

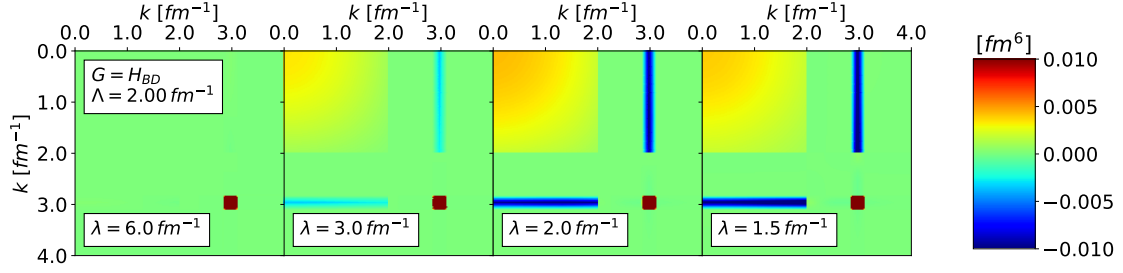


(b)

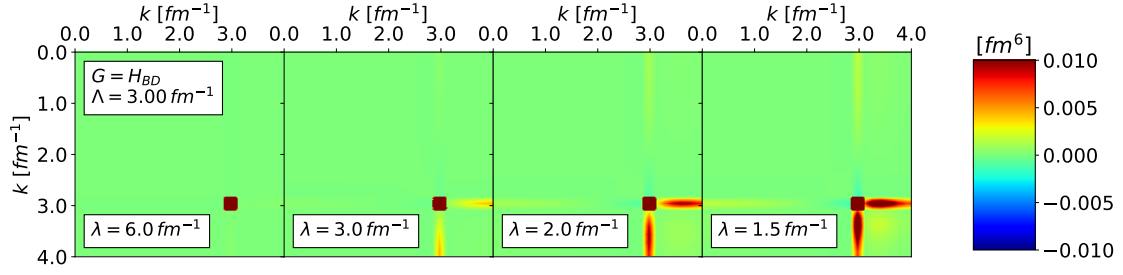
FIG. 16: Matrix elements of the Gezerlis et al.  $N^2\text{LO}$  local potential  $V_\lambda(k, k')$  SRG-evolving in  $\lambda$  right to left under transformations with the Wegner generator (a) and block-diagonal generator decoupling at  $\Lambda = 2 \text{ fm}^{-1}$  (b). Here the EFT cutoff is  $1.2 \text{ fm}$ .



(a)



(b)



(c)

FIG. 17: Matrix elements of  $\langle k|a_q^\dagger a_q|k'\rangle$  SRG-evolving in  $\lambda$  right to left under transformations from the Gezerlis et al. N<sup>2</sup>LO local potential with the Wegner generator (a) and block-diagonal generators decoupling at  $\Lambda = 2$  and  $3 \text{ fm}^{-1}$  (b and c). Here  $q = 3 \text{ fm}^{-1}$  and the EFT cutoff is  $1 \text{ fm}$ .

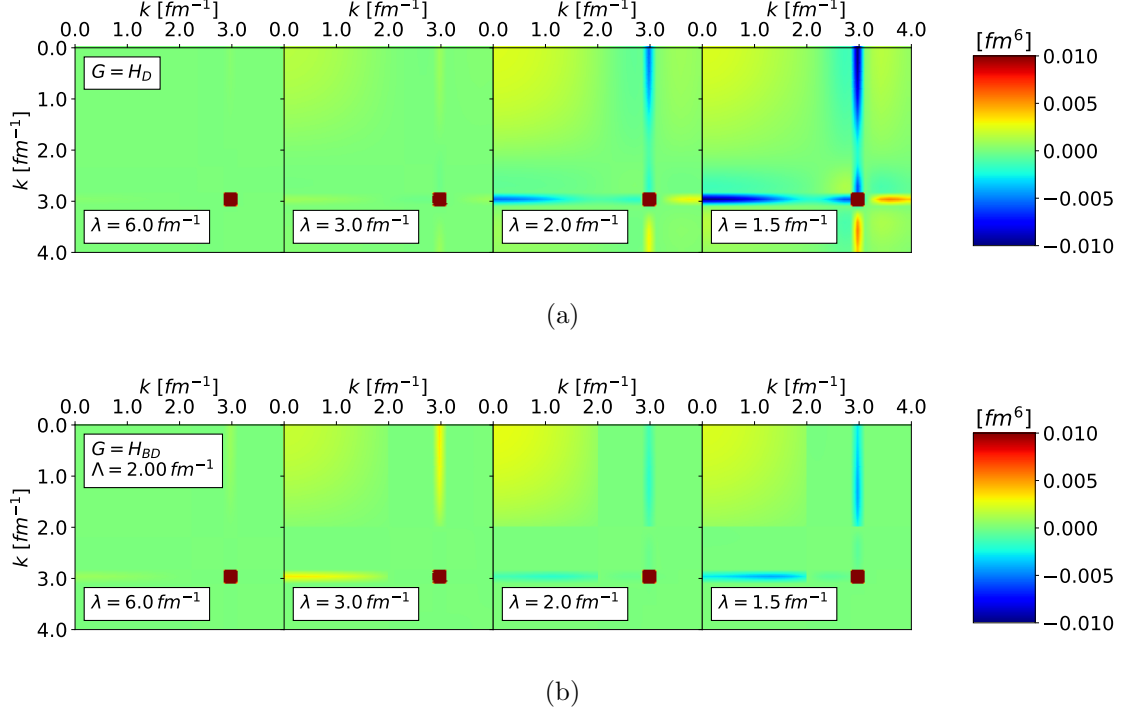


FIG. 18: Matrix elements of  $\langle k|a_q^\dagger a_q|k' \rangle$  SRG-evolving in  $\lambda$  right to left under transformations from the Gezerlis et al.  $N^2\text{LO}$  local potential with the Wegner generator (a) and block-diagonal generator decoupling at  $\Lambda = 2 \text{ fm}^{-1}$  (b). Here  $q = 3 \text{ fm}^{-1}$  and the EFT cutoff is  $1.2 \text{ fm}$ .

- 
- [1] D. R. Entem and R. Machleidt, Phys. Rev. C **68**, 041001 (2003), arXiv:nucl-th/0304018 [nucl-th].
  - [2] E. R. Anderson, S. K. Bogner, R. J. Furnstahl, and R. J. Perry, Phys. Rev. C **82**, 054001 (2010), arXiv:1008.1569 [nucl-th].
  - [3] P. Reinert, H. Krebs, and E. Epelbaum, Eur. Phys. J. A **54**, 86 (2018), arXiv:1711.08821 [nucl-th].
  - [4] A. Gezerlis, I. Tews, E. Epelbaum, M. Freunek, S. Gandolfi, K. Hebeler, A. Nogga, and A. Schwenk, Phys. Rev. C **90**, 054323 (2014), arXiv:1406.0454 [nucl-th].